Dielectronic capture processes in the electron-impact ionization of Sc^{2+}

M. S. Pindzola and T. W. Gorczyca
Department of Physics, Auburn University, Auburn, Alabama 36849

N. R. Badnell
Department of Physics & Applied Physics, University of Strathclyde, Glasgow G4 ONG, United Kingdom

D. C. Griffin
Department of Physics, Rollins College, Winter Park, Florida 32749

M. Stenke, G. Hofmann, B. Weissbecker, K. Tinschert,* and E. Salzborn
Institut fur Kernphysik, Universitat Giessen, D-35392 Giessen, Federal Republic of Germany

A. Müller
Institut fur Strahlenphysik, Universitat Stuttgart, D-70550 Stuttgart, Federal Republic of Germany

G. H. Dunn
Joint Institute for Laboratory Astrophysics, Boulder, Colorado 80309
(Received 14 September 1993)

Theoretical and experimental results are presented for the electron-impact ionization of Sc^{2+} in the near-threshold energy region where strong resonance features due to dielectronic capture processes are found. The indirect ionization contributions are calculated in the close-coupling approximation. Both absolute and scan measurements for the ionization cross section are obtained in a crossed-beams experimental geometry. The overall agreement between theory and experiment is good, once a sufficient number of singly excited states are included in the close-coupling expansion. The additional states allow a proper theoretical determination of the decay pathways available to the resonances formed following dielectronic capture of the incident electron.

PACS number(s): 34.80.Kw

I. INTRODUCTION

It is quite common to find large indirect electron-impact ionization processes for those atomic ions whose electronic structure consists of one or two electrons outside a closed subshell containing six or more electrons [1]. Basically, the direct ionization of the few outer electrons is overwhelmed by a strong rate for electron-impact excitation of autoionizing states from the many electrons of the inner subshell. The atomic ions of the Na-like isoelectronic sequence, with a ground configuration of $2p^6 3s$, provide a well-studied example [2–13]. From Si^{3+} to U^{81+} the indirect ionization processes are generally 1–10 times larger than the direct ionization of the $3s$ electron in the near-threshold energy region. The principal indirect ionization mechanisms are excitation followed by single autoionization and dielectronic capture followed by the sequential autoionization of two electrons. For Fe^{15+} the dielectronic-capture process itself enhances the collisional ionization rate by 30% for temperatures near the ionization potential [10].

In this paper we present both theoretical and experimental results for the electron-impact ionization of Sc^{2+}. With a ground configuration of $3p^6 3d$, we expect large indirect ionization contributions. Unlike studies [14,15] of Ca^+, the principal autoionizing configuration of $3p^5 3d^2$ in Sc^{2+} is not complicated by the presence of LS term dependence. Also, unlike studies [16–19] of Ti^{3+}, the $3p^5 3d^2$ configuration does not straddle the ionization threshold, so that all 19 LS terms of the configuration contribute to the excitation-autoionization process. Since Sc^{2+} has a low residual charge (Z), the effects of radiation damping on resonance decays should be minimal; they scale as Z^4 and are only important for more highly charged ions. Thus the indirect ionization contributions for Sc^{2+} are readily calculable in the nonperturbative close-coupling approximation. The comparison with high-resolution crossed-beams measurements for Sc^{2+} provides an opportunity for a detailed examination of the sensitivity of the dielectronic capture processes to the number and type of states included in the close-coupling expansion. We present a brief theoretical summary in Sec. II, a description of the crossed-beams experimental method in Sec. III, a comparison of theory and experiment in Sec. IV, and provide conclusions in Sec. V.

II. THEORY

In the independent-processes approximation the total ionization cross section $\sigma_t(i \rightarrow f)$ is given by

*Present address: GSI, D-64220 Darmstadt, Federal Republic of Germany.

$$\sigma_t(i\rightarrow f)=\sigma_d(i\rightarrow f)+\sum_n \sigma_x(i\rightarrow n)\frac{A_a(n\rightarrow f)}{\Gamma_n} , \quad (1)$$

where $\sigma_d(i\rightarrow f)$ is the direct ionization cross section, $\sigma_x(i\rightarrow n)$ is the direct and resonant excitation cross section to an autoionizing state n, $A_a(n\rightarrow f)$ is the Auger transition rate, and Γ_n is the total decay rate. Direct ionization for the dominant configuration of ground state Sc^{2+} proceeds via the reaction

$$e^- + Sc^{2+}(3p^6 3d)\rightarrow Sc^{3+}(3p^6)+2e^- . \quad (2)$$

A configuration-average distorted-wave method [20], employing a triple partial-wave expansion of the first-order perturbation-theory scattering amplitude, is used to calculate σ_d for the $3d$ subshell. At higher energies the $3p$ and $3s$ subshells also contribute to the direct ionization cross section.

The largest indirect ionization cross section contributions are due to excitation of Sc^{2+} via the reaction

$$e^- + Sc^{2+}(3p^6 3d\ ^2D)\rightarrow Sc^{2+}(3p^5 3d^2 LS)+e^- . \quad (3)$$

All 19 LS terms of the $3p^5 3d^2$ configuration may autoionize to the $3p^6\ ^1S$ continuum in which they lie embedded via the reaction

$$Sc^{2+}(3p^5 3d^2 LS)\rightarrow Sc^{3+}(3p^6\ ^1S)+e^- . \quad (4)$$

The branching ratio for autoionization, $A_a(n\rightarrow f)/\Gamma_n$ in Eq. (1), may be set to 1 for almost all doubly charged ions. Both an LS close-coupling and an LS distorted-wave method are used to calculate σ_x for the $3p\rightarrow 3d$ transition.

The Opacity Project version of the R-matrix codes [21] has been suitably modified to provide both target eigenfunctions and collision algebra to a separate unitarized distorted-wave code [22]. In this way continuum coupling effects on the nonresonant part of the excitation cross section may be easily determined.

Dielectronic-capture contributions to the total ionization cross section proceed via the reaction

$$e^- + Sc^{2+}(3p^6 3d\ ^2D)\rightarrow Sc^{+}(3p^5 3d^2 L'S'nl) . \quad (5)$$

The dielectronic-capture resonances contribute to ionization via an LS multiplet-changing autoionizing decay:

$$Sc^{+}(3p^5 3d^2 L'S'nl)\rightarrow Sc^{2+}(3p^5 3d^2 LS)+e^- , \quad (6)$$

sequentially followed by the autoionizing decay of Eq. (4). The dielectronic-capture resonances may also autoionize to bound states of Sc^{2+}, and thus fail to contribute to ionization, via the reactions

$$Sc^{+}(3p^5 3d^2 L'S'nl)\rightarrow Sc^{2+}(3p^6 3d\ ^2D)+e^- , \quad (7)$$

and

$$Sc^{+}(3p^5 3d^2 L'S'nl)\rightarrow Sc^{2+}(3p^6 nl\ ^2l)+e^- . \quad (8)$$

The core-rearrangement autoionizing decay of Eq. (8) is noteworthy in that its rate is independent of the spectator nl orbital for high n. An LS close-coupling calculation for the $3p\rightarrow 3d$ excitation automatically includes contributions from dielectronic capture resonances through coupling to energetically closed channels. It is important to include a sufficient number of both singly excited ($3p^6 nl\ ^2l$) and doubly excited ($3p^5 3d^2 LS$) terms in the close-coupling expansion to allow the resonance states to properly decay [23].

The dielectronic-capture contribution to the total ionization cross section may also be calculated in an LS distorted-wave method if one extends the independent-processes approximation to separate the resonances from the excitation background in the determination of $\sigma_x(i\rightarrow n)$. Interference effects, which are naturally included in the close-coupling method, are thus ignored. Recent close-coupling and distorted-wave calculations of resonance structures in the excitation of low-lying excited bound states of Na-like ions [24] are in good agreement for high ionization stages. For low ionization stages, however, the interference between the direct and resonant excitation processes leads to window features in the total cross section. Further close-coupling and distorted-wave comparisons for Mg-like ions [25] have also found sizable effects on resonance structures due to an apparent breakdown of the isolated-resonance approximation. Thus we only carried out close-coupling calculations for the dielectronic-capture processes in Sc^{2+}.

III. EXPERIMENT

The experimental data were collected using the Giessen electron-ion crossed-beams apparatus. The present setup was recently described in detail [26]. The Sc^{2+} ions were produced in a Penning ion source using sputter techniques. The acceleration voltage for the ions was 10 kV. The ion beam was magnetically analyzed and tightly collimated before entering the collision region. It was crossed with an intense ribbon-shaped electron beam. The ionized (Sc^{3+}) ions were magnetically separated from the parent Sc^{2+} beam and registered by a single-particle counter. The parent beam was collected by a large Faraday cup.

Two modes of data taking were employed to study ionization cross sections.

Mode 1: Absolute ionization cross sections were obtained by employing a technique [27,28] wherein the electron gun is moved up and down across the ion beam while the counting rate of ionized ions [spectrum (1)], the ion current [spectrum (2)], and the electron current [spectrum (3)] are recorded simultaneously as three different multichannel analyzer (MCA) spectra with 512 channels each. In a fourth MCA spectrum the pulses of a fixed-frequency pulser are recorded providing the dwell time per channel (and hence also the speed of the electron beam displacement).

When the two beams cross each other the observed counting rate is increased by the true ionization signal, leading to a peak in the spectrum. In the extreme positions of the electron gun the beams do not overlap and hence the observed counting rate gives the experimental background, which is mostly due to stripping collisions in the residual gas. For the determination of an absolute cross section a fifth MCA spectrum is calculated where the content of channel j is given by $N_j^{(1)}N_j^{(4)}/(N_j^{(2)}N_j^{(3)})$.

The quantities $N_j^{(1)}$, $N_j^{(2)}$, $N_j^{(3)}$, and $N_j^{(4)}$ are the contents of the first four spectra in their channel j and correspond to the instantaneous signal, ion charge, electron charge, and dwell time.

The fifth spectrum shows a peak when there is overlap of the two beams and when ionized ions can be detected. From the area S of the peak in the spectrum (after background subtraction) the cross section is calculated using

$$\sigma=\frac{S\Delta}{M\epsilon}K \ . \tag{9}$$

The constant K contains the conversion factors of beam currents to proportional frequencies and the frequency of the time pulses; ϵ is the detection efficiency of the single particle detector for the product ions. Each channel of the MCA spectra corresponds to a position interval $\Delta=0.036$ mm. The dwell time per interval Δ for a single movement of the electron gun across the beam is about 0.1 s. The factor M is given by

$$M=(v_e^2+v_i^2)/(v_e v_i q e^2) \ . \tag{10}$$

Here, v_e is the electron velocity, v_i is the ion velocity, q is the target ion charge state, and e is the charge of an electron.

Mode 2: For the measurement of fine details of the ionization cross section we have employed a data-taking mode [29] providing for fast energy scans with the electron gun in a fixed position, i.e., with fixed overlap of the electron and ion beams. On a computer, a digital-to-analog converter was programmed to output a step function with up to 4096 individual voltages. This step function was used with variable offset and amplification to control the energy of the electrons in the interaction region. Changing the energy and providing the necessary gate signals took about 300 μs. As a compromise between scan speed and efficient data collection, we chose a dwell time of 3 ms on each electron energy and a step width of 0.039 eV. The scan showing most of the cross section structures spanned about 50 eV and took a little over 4 s for about 1300 data points. By repeating scans thousands of times, it was possible to average out fluctuations in the beam overlap (usually expressed in terms of a form factor) [1], fluctuations in the measured beam currents, counting rates, and in other sources of data scatter.

Earlier experiments [13,29] employing the Giessen setup and the techniques briefly discussed above have demonstrated an electron energy spread of 0.4 eV or better in the energy range below 100 eV. In the present experiment we accumulated up to about 10^5 signal counts per channel and thus reduced the minimum statistical uncertainty to the 0.3–0.4 % level. This is sufficient to visualize all the Sc^{2+} ionization cross section details which are detectable with the present energy resolution.

Although the point-to-point uncertainty in the relative scan measurements (mode 2) is very low, the absolute uncertainty is limited by the absolute cross-section measurements (mode 1). In the scanning mode we do not have direct information about the form factor which determines the beam overlap. Also, the background is measured in separate runs with no overlap of the electron and ion beams. Time spans between the measurement of signal plus background and only background may be hours, so that an exact background subtraction cannot be guaranteed. A false subtraction of background, however, does not introduce spurious structure since the background spectra (versus energy) are completely flat or, at most, slightly increasing with the electron current. Resulting uncertainties in the scan cross sections are substantially eliminated by normalizing them to the absolute measurements (mode 1). For the present experiments, normalization just meant the multiplication of all scan data with a constant factor to match them with the absolute cross-section points. After all of these procedures, the absolute uncertainties of the scan data are close to those of the conventional measurements (mode 1), i.e., 7.8% systematic uncertainty plus statistical uncertainties of the single measurement which are lower than 1%.

The cross section measurements displayed in the figures consist of several individual scans. When tying overlapping scans together the statistical uncertainty of cross sections in the overlap region is, of course, smaller (by about a factor of $\sqrt{2}$) than that in the remaining scanning regions. Also, different scan intervals were given different data accumulation times, depending on the structures in the cross section to be detected. Hence the statistical uncertainties of cross-section data displayed in the following figures may vary with electron energy.

IV. RESULTS

Figure 1 shows the experimental scan data (mode 2) together with absolute cross sections (mode 1) for single ionization of Sc^{2+}. The error bars on the absolute cross sections represent the total uncertainty of each single measurement. The scan data are shown as small vertical bars the length of which represents the statistical uncertainty. The ionization energy of ground-state Sc^{2+} is 24.76 eV according to Moore [30].

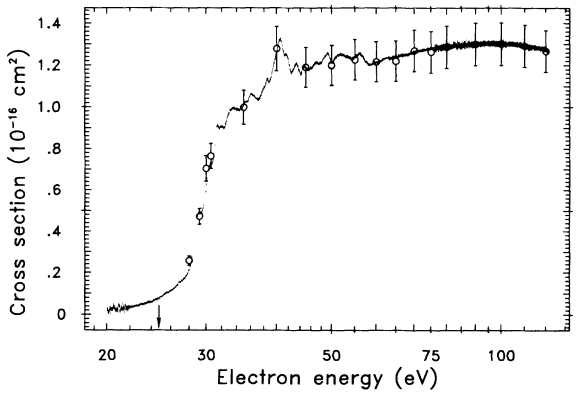

FIG. 1. Experimental cross sections for net single ionization of Sc^{2+} ions. The scan data (mode 2, see text) are indicated by their statistical error bars (typically only 0.3–0.4 % near the cross-section maximum). The absolute cross-section measurements (mode 1, see text) are represented by the open circles together with the total experimental uncertainty of each single data point. The ionization threshold of ground-state Sc^{2+} is indicated by a vertical arrow.

The experimental scan data show a relatively smooth onset of the cross section which does not exhibit the normal signature of a clear-cut ionization threshold. The measured cross section rather indicates the presence of a small fraction of metastable species possibly from different excited states. As a consequence the direct ionization cross section below the $3p^5 3d^2$ excitation threshold is higher than expected for a beam of ground-state Sc^{2+} parent ions. With increasing electron energy metastable and ground-state ions may behave differently, which leaves a small uncertainty in the correct description of the experimental data. We believe, however, that this effect is not larger than the total experimental uncertainty.

The radial orbitals for all subsequent distorted-wave and close-coupling calculations were generated in a single-configuration Hartree-Fock approximation [31] for the $3p^6 nl$ ground and excited configurations of Sc^{2+}. The Hartree-Fock energies for the 19 *LS* terms of the $3p^5 3d^2$ configuration are given in Table I. It was found earlier [32] that using the atomic structure code of Cowan [33] one could obtain good agreement with experimental energies for the bound states of $3p^5 3d^2$ in the isoelectronic ion V^{4+} by scaling the electrostatic Slater parameters by a factor of 0.80 to correct for correlation effects. As shown in Table I, the scaled Hartree-Fock energies for Sc^{2+} are in overall agreement with the Hartree-Fock energies, but differences of 1–2 eV are found.

Configuration-average ionization and excitation cross sections [20] for Sc^{2+} are presented in Table II. Direct ionization from all the $n=3$ subshells contributes to the single ionization cross section. The configuration-average distorted-wave calculations show that excitation to the $3p^5 3d^2$ configuration is an order of magnitude stronger than the excitation to the $3p^5 3d4l$ configurations. Thus we limited our subsequent *LS*-term close-coupling and distorted-wave calculations to the strong $3p^6 3d\ ^2D \rightarrow 3p^5 3d^2 LS$ transitions.

TABLE I. Energy levels for Sc^{2+}.

LS term		Hartree-Fock energies (eV)	Scaled Hartree-Fock energies (eV)
$3p^6 3d$	^2D	0.00	0.00
$3p^5 3d^2(^3F)$	^4D	27.11	28.08
$3p^5 3d^2(^3F)$	^4G	28.75	29.42
$3p^5 3d^2(^3P)$	^4P	28.78	29.45
$3p^5 3d^2(^3F)$	^4F	29.73	30.22
$3p^5 3d^2(^1D)$	^2D	29.90	30.36
$3p^5 3d^2(^1G)$	^2F	30.05	30.48
$3p^5 3d^2(^1D)$	^2P	30.61	30.95
$3p^5 3d^2(^1G)$	^2H	31.14	31.38
$3p^5 3d^2(^3F)$	^2G	31.46	31.63
$3p^5 3d^2(^1D)$	^2F	31.50	31.66
$3p^5 3d^2(^3P)$	^4D	32.14	32.19
$3p^5 3d^2(^3P)$	^2D	33.60	33.38
$3p^5 3d^2(^3P)$	^2S	33.94	33.66
$3p^5 3d^2(^3P)$	^4S	33.94	33.66
$3p^5 3d^2(^1G)$	^2G	34.08	33.78
$3p^5 3d^2(^1S)$	^2P	35.70	35.11
$3p^5 3d^2(^3F)$	^2F	39.61	38.26
$3p^5 3d^2(^3P)$	^2P	43.16	41.19
$3p^5 3d^2(^3F)$	^2D	44.35	42.15

TABLE II. Configuration-average ionization and excitation cross sections for electron impact on Sc^{2+}.

Subshell	Ionization energy (eV)	Cross section at twice threshold (10^{-18} cm^2)
	Ionization	
$3d$	24.62	26.80
$3p$	57.17	20.07
$3s$	84.50	2.84
	Excitation	
Transition	Excitation energy (eV)	Cross section at threshold (10^{-18} cm^2)
$3p \rightarrow 3d$	32.01	287.97
$3p \rightarrow 4s$	35.46	5.30
$3p \rightarrow 4p$	40.03	22.89
$3p \rightarrow 4d$	46.25	11.64
$3p \rightarrow 4f$	49.30	0.88

Comparisons between close-coupling calculations, distorted-wave calculations, and experiment are made in Figs. 2–4. In all the figures there is good agreement between the close-coupling and distorted-wave calculations for the excitation-autoionization contributions. This is somewhat surprising since this is not the case for the neighboring Ca^+ ion [15]. Close-coupling calculations including $3p^6 3d\ ^2D$, $3p^6 4s\ ^2S$, and the 19 *LS* terms of $3p^5 3d^2$ are compared with the experimental measurements in Fig. 2. The dielectronic-capture resonances are spread over the 17-eV difference between the lowest- and

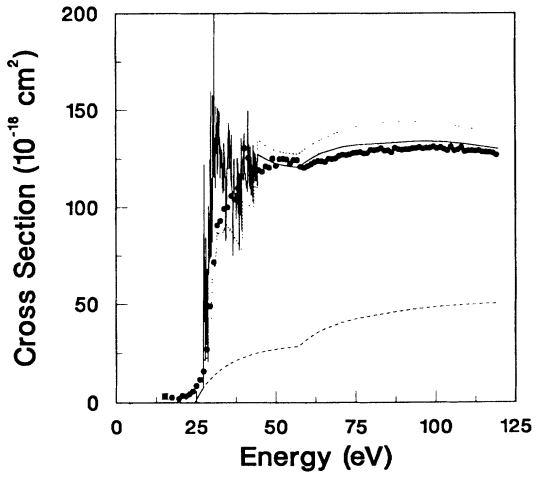

FIG. 2. Electron-impact ionization of Sc^{2+}. Dashed curve: configuration-average distorted-wave calculations for the $3d$, $3p$, and $3s$ subshells. Solid curve: 21-*LS*-term close-coupling calculation for excitation-autoionization and resonant-excitation double autoionization contributions plus direct. Dotted curve: 21-*LS*-term unitarized distorted-wave calculation for excitation-autoionization contributions plus direct. Solid circles: experimental crossed-beams measurements at every 20th point.

highest-energy terms of the $3p^5 3d^2$ configuration. The 21-term close-coupling calculations yield resonance structures with generally larger cross sections than experiment, especially in the energy region around 32 eV.

We probed the effect of core-rearrangement decay channels [see Eq. (8)] by extending the 21-term close-coupling calculation to include five more terms: $3p^6 4p\ ^2P$, $3p^6 4d\ ^2D$, $3p^6 4f\ ^2F$, $3p^6 5s\ ^2S$, and $3p^6 5p\ ^2P$. As shown in Fig. 3, there is a very noticeable decrease in the strength of the dielectronic-capture resonances and thus improved agreement with experiment. It becomes increasingly difficult to include more $3p^6 nl\ ^2l$ terms in the close-coupling expansion, since the R-matrix boundary must be enlarged to make room for the subsequent Rydberg orbitals. Dielectronic-ionization distorted-wave methods [11,24] may also be used to help resolve the convergence problems associated with the core-rearrangement decay channels.

Finally, in Fig. 4, we compare theory and experiment on an expanded energy scale in the resonance region. Two close-coupling results are presented, both convoluted with a 0.4-eV full-width-at-half-maximum (FWHM) Gaussian to simulate the energy resolution of the electron beam. The solid curve in Fig. 4 is a 26-state calculation with Hartree-Fock energies, and the chained curve is a 26-state calculation employing scaled Hartree-Fock energies. The close-coupling results with scaled Hartree-Fock energies line up better with the experimental onsets of excitation-autoionization features. The 21-state unitarized distorted-wave calculations (dotted curve) are also included in the figure to delineate the 19-LS-term excitation thresholds for $3p^5 3d^2$. The largest difference between theory and experiment is found around 32 eV. This is precisely the energy region that saw the largest decrease in the resonance structure strength when further core-rearrangement decay channels were included.

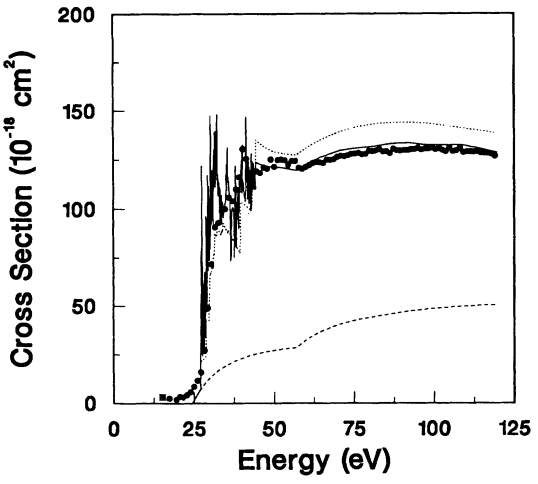

FIG. 3. Electron-impact ionization of Sc^{2+}. Dashed curve: configuration-average distorted-wave calculations for the 3d, 3p, and 3s subshells. Solid curve: 26-LS-term close-coupling calculation for excitation autoionization and resonant-excitation double autoionization contributions plus direct. Dotted curve: 21-LS-term unitarized distorted-wave calculation for excitation-autoionization contributions plus direct. Solid circles: experimental crossed-beams measurements at every 20th point.

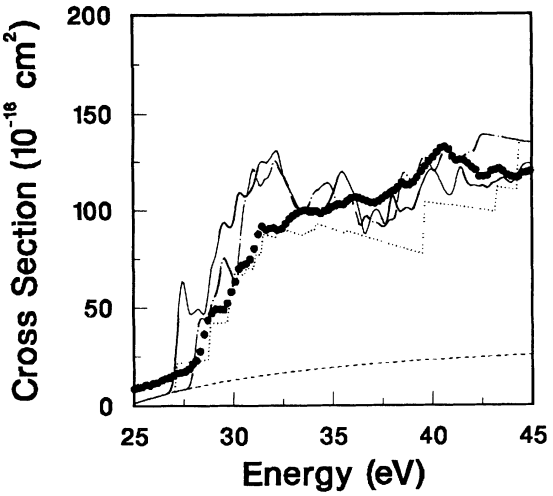

FIG. 4. Electron-impact ionization of Sc^{2+}. Dashed curve: configuration-average distorted-wave calculations for the 3d, 3p, and 3s subshells. Solid curve: 26-LS-term close-coupling calculation for excitation-autoionization and resonant-excitation double autoionization contributions plus direct, convoluted with a 0.4-eV FWHM Gaussian. Chained curve: 26-LS-term close-coupling calculation for excitation-autoionization and resonant-excitation double autoionization contributions plus direct, convoluted with a 0.4-eV FWHM Gaussian, and using scaled Hartree-Fock energies. Dotted curve: 21-LS-term unitarized distorted-wave calculation for excitation-autoionization contributions plus direct. Solid circles: experimental crossed-beams measurements at every fifth point.

Complicating the detailed comparison between theory and experiment shown in Fig. 4 are a variety of effects, each at probably the 10–20% level. As stated earlier, the experiment may be reporting a $3p^6 3d$ ionization cross section mixed with a small fraction of $3p^6 4s$ metastable ionization. The theory does not include electron correlation effects on the excitation cross sections and resonance profiles, only on the threshold energies through the use of scaling parameters. Finally, theory does not include the relatively small $3p \rightarrow 4l$ excitation-autoionization contributions and the resonance structures which may be attached to their higher excitation thresholds.

V. CONCLUSIONS

We have completed a joint theoretical and experimental study of the electron-impact ionization of Sc^{2+} in the near-threshold region. A 26-LS-term close-coupling calculation for the $3p^6 3d\ ^2D \rightarrow 3p^5 3d^2\ LS$ transitions, incoherently added to a configuration-average distorted-wave calculation for direct ionization of the $n=3$ subshells, is in good agreement with the high-resolution crossed-beams measurements over most of the energy range. By comparing 21- and 26-LS-term close-coupling calculations, we find that core-rearrangement autoionizing decay channels have a strong influence on the dielectronic-capture resonance structure. Once folded with a 0.4-eV FWHM Gaussian, and shifted slightly in energy through the use of scaled Hartree-Fock energies,

many resonance features in the theoretical and experimental spectrums line up fairly well. For certain resonance features, however, there remains a noticeable disagreement between theory and experiment.

ACKNOWLEDGMENTS

We would like to thank the members of the Opacity Project for providing us with the latest versions of the *R*-matrix programs. This work was supported by the U.S. Department of Energy under Contract No. DE-FG05-86ER53217 with Auburn University, under Contract No. DE-AC05-84OR21400 with Martin Marietta Energy Systems, Inc., contract operator of Oak Ridge National Laboratory, and under Contract No. DE-A105-86ER53237 with the National Institute of Standards and Technology. Support was also provided by Deutsche Forschungsgemeinschaft (DFG), Bonn-Bad Godesberg, and through NATO Collaborative Research Grant No. RG 86/0510.

[1] A. Müller, in *Physics of Ion Impact Phenomena,* edited by D. Mathur, Springer Series in Chemical Physics Vol. 54 (Springer-Verlag, Berlin, 1991), pp. 13–90.

[2] D. H. Crandall, R. A. Phaneuf, R. A. Falk, D. S. Belić, and G. H. Dunn, Phys. Rev. A **25**, 143 (1982).

[3] D. C. Griffin, C. Bottcher, and M. S. Pindzola, Phys. Rev. A **25**, 154 (1982).

[4] R. J. W. Henry and A. Z. Msezane, Phys. Rev. A **26**, 2545 (1982).

[5] Y. Zhang, C. B. Reddy, R. S. Smith, D. E. Golden, D. W. Mueller, and D. C. Gregory, Phys. Rev. A **45**, 2929 (1992).

[6] D. C. Gregory, L. J. Wang, F. W. Meyer, and K. Rinn, Phys. Rev. A **35**, 3256 (1987).

[7] K. J. LaGattuta and Y. Hahn, Phys. Rev. A **24**, 2273 (1981).

[8] D. C. Griffin, M. S. Pindzola, and C. Bottcher, Phys. Rev. A **36**, 3642 (1987).

[9] S. S. Tayal and R. J. W. Henry, Phys. Rev. A **39**, 3890 (1989).

[10] M. H. Chen, K. J. Reed, and D. L. Moores, Phys. Rev. Lett. **64**, 1350 (1990).

[11] M. H. Chen and K. J. Reed, Phys. Rev. A **47**, 1874 (1993).

[12] K. J. Reed, M. H. Chen, and D. L. Moores, Phys. Rev. A **44**, 4336 (1991).

[13] A. Müller, G. Hofmann, K. Tinschert, B. Weissbecker, and E. Salzborn, Z. Phys. D **15**, 145 (1990).

[14] B. Peart, J. R. A. Underwood, and K. Dolder, J. Phys. B **22**, 2789 (1989).

[15] N. R. Badnell, D. C. Griffin, and M. S. Pindzola, J. Phys. B **24**, L275 (1991).

[16] R. A. Falk, G. H. Dunn, D. C. Griffin, C. Bottcher, D. C. Gregory, D. H. Crandall, and M. S. Pindzola, Phys. Rev. Lett. **47**, 494 (1981).

[17] C. Bottcher, D. C. Griffin, and M. S. Pindzola, J. Phys. B **16**, L65 (1983).

[18] P. G. Burke, W. C. Fon, and A. E. Kingston, J. Phys. B **17**, L733 (1984).

[19] D. C. Griffin, M. S. Pindzola, and N. R. Badnell, J. Phys. B **24**, L621 (1991).

[20] M. S. Pindzola, D. C. Griffin, and C. Bottcher, in *Atomic Processes in Electron-Ion and Ion-Ion Collisions,* Vol. 145 of *NATO Advanced Study Institute Series B: Physics,* edited by F. Brouillard (Plenum, New York, 1986), p. 75.

[21] K. A. Berrington, P. G. Burke, K. Butler, M. J. Seaton, P. J. Storey, K. T. Taylor, and Y. Yan, J. Phys. B **20**, 6379 (1987).

[22] M. S. Pindzola, D. C. Griffin, and C. Bottcher, Phys. Rev. A **39**, 2385 (1989).

[23] The effect of singly excited states on the excitation cross section to $3p^5 3d^2$ in Ti^{3+} is demonstrated and discussed in Ref. [19]. However, it should be noted that in performing the calculation of the $3p^6 \rightarrow 3p^5 3d^2$ transition in Sc^{2+}, we discovered that several *LS* Π symmetries had been mistakenly omitted from the close-coupling expansion for this transition in Ti^{3+}. This has a significant effect on the magnitude of several of the cross sections. We are in the process of repeating the calculations for Ti^{3+}, including the effects of increased correlation.

[24] N. R. Badnell, M. S. Pindzola, and D. C. Griffin, Phys. Rev. A **43**, 2250 (1991).

[25] N. R. Badnell, D. C. Griffin, T. W. Gorczyca, and M. S. Pindzola, Phys. Rev. A **48**, 2519 (1993).

[26] K. Tinschert, A. Müller, G. Hofmann, K. Huber, R. Becker, D. C. Gregory, and E. Salzborn, J. Phys. B **22**, 531 (1989).

[27] A. Müller, K. Huber, K. Tinschert, R. Becker, and E. Salzborn, J. Phys. B **14**, 2993 (1985).

[28] A. Müller, K. Tinschert, C. Achenbach, E. Salzborn, and R. Becker, Nucl. Instrum. Methods Phys. Res. B **24/25**, 369 (1987).

[29] A. Müller, K. Tinschert, G. Hofmann, E. Salzborn, and G. H. Dunn, Phys. Rev. Lett. **61**, 70 (1988).

[30] C. E. Moore, *Atomic Energy Levels,* Natl. Stand. Ref. Data Ser., Natl. Bur. Stand. (U.S.) Circ. No. 34 (U.S. GPO, Washington, DC, 1970).

[31] C. F. Fischer, Comput. Phys. Commun. **64**, 369 (1991).

[32] D. C. Griffin, C. Bottcher, and M. S. Pindzola, Phys. Rev. A **25**, 1374 (1982).

[33] R. D. Cowan, *The Theory of Atomic Structure and Spectra* (University of California Press, Berkeley, 1981).